Supporting Information

The Direct Synthesis of Hydrogen Peroxide from H_2 and O_2 Using Pd-Ga and Pd-In Catalysts

Sheng Wang [a,b], Richard J. Lewis [c], Dmitry E. Doronkin [a,d], David J. Morgan [c], Michael Zimmermann [a], Jan-Dierk Grunwaldt [a,d], Graham J. Hutchings [c], Silke Behrens [a,b*]*

[a] Institute of Catalysis Research and Technology (IKFT), Karlsruhe Institute of Technology (KIT), Hermann-von-Helmholtz-Platz 1,76344 Eggenstein-Leopoldshafen, Germany.

[b] Institute of Inorganic Chemistry, Ruprecht-Karls University Heidelberg, Im Neuenheimer Feld 270, 69120 Heidelberg, Germany

[c] Cardiff Catalysis Institute, School of Chemistry, Cardiff University, Main Building, Park Place, Cardiff, CF10 3AT, United Kingdom.

[d] Institute for Chemical Technology and Polymer Chemistry (ITCP), Karlsruhe Institute of technology (KIT), Engesserstr. 20, 76131 Karlsruhe, Germany.

Table S.1. Reaction conditions used in this work for the synthesis of nanoparticles and molar elemental compositions obtained by ICP-OES analysis.

Nanoparticles	Metal Precursors	Pd:M (precursors molar ratio)	TOP (mL)	OLAM (mL)	Temperature (°C)	Composition (molar ratio)
Pd	$Pd(acac)_2$		2	40	200	Pd1
Pd2Ga	$Pd(acac)_2$ $Ga(acac)_3$	2:1	2	40	300	$Pd_{0.77}Ga_{0.23}$
Pd1Ga	$Pd(acac)_2$ $Ga(acac)_3$	1:1	2	40	300	$Pd_{0.48}Ga_{0.52}$
Pd0.5Ga	$Pd(acac)_2$ $Ga(acac)_3$	1:2	2	40	300	$Pd_{0.38}Ga_{0.62}$
Ga	$Ga(acac)_3$		2	40	330	Ga1
Pd2In	$Pd(acac)_2$ $In(acac)_3$	2:1	2	40	300	$Pd_{0.78}In_{0.22}$
Pd1In	$Pd(acac)_2$ $In(acac)_3$	1:1	2	40	300	$Pd_{0.66}In_{0.34}$
Pd0.5In	$Pd(acac)_2$ $In(acac)_3$	1:2	2	40	300	$Pd_{0.49}In_{0.51}$
In	$In(acac)_3$		2	40	300	In1

Table S.2. Monometallic Pd, Ga, In and bimetallic Pd-Ga and Pd-In supported catalysts' elemental composition obtained by ICP-OES analysis.

Catalysts	Pd loading (wt.%)	M loading (wt. %)	PdM loading (wt. %)	Composition (molar ratio)
Pd/TiO_2	5.6	-	5.6	Pd1
$Pd2Ga/TiO_2$	2.64	0.56	3.2	$Pd_{0.76}Ga_{0.24}$
$Pd1Ga/TiO_2$	3.93	1.31	5.2	$Pd_{0.66}Ga_{0.34}$
$Pd0.5Ga/TiO_2$	2.41	1.67	4.1	$Pd_{0.49}Ga_{0.51}$
Ga/TiO_2	-	4.1	4.1	Ga1
$Pd2In/TiO_2$	3.88	1.13	5.0	$Pd_{0.78}In_{0.22}$
$Pd1In/TiO_2$	2.85	1.14	4.0	$Pd_{0.73}In_{0.27}$

Pd0.5In/TiO_2	2.35	1.15	3.5	$Pd_{0.69}In_{0.31}$
In/TiO_2	-	4.04	4.04	In1

Table S.3. Particle size of as-prepared, unsupported and supported Pd-Ga and Pd-In nanoparticles as a function of Pd : M (M= Ga,In) ratio determined by TEM.

Catalyst	Particle size / nm (Standard deviation)	
	Unsupported Nanoparticles	Supported Nanoparticles
Pd/TiO_2	4.8 (0.5)	4.1 (1.6)
Pd2Ga/TiO_2	3.5 (0.4)	3.6 (1.9)
Pd1Ga/TiO_2	4.4 (0.7)	4.3 (1.0)
Pd0.5Ga/TiO_2	5.4 (0.7)	4.9 (1.1)
Pd2In/TiO_2	5.7 (0.8)	3.6 (1.7)
Pd1In/TiO_2	5.2 (0.9)	4.4 (1.5)
Pd0.5In/TiO_2	2.9 (0.5)	2.3 (0.9)

Table S.4. Results of EXAFS analysis for Pd, Pd-Ga and Pd-In supported catalysts.

Supported catalysts	d Pd-O (Å)	CN (O)	σ^2 (O) (10^{-3} Å^2)	d Pd-M (Å)	CN (M)	σ^2 (M) (10^{-3} Å^2)	d Pd-Pd (Å)	CN (Pd)	σ^2 (Pd) (10^{-3} Å^2)	δE_0 (eV)	ρ (%)
Pd foil	-	-	-	-	-	-	2.737±0.002	12*	4.6±0.4	-3.1±0.4	0.5
Pd/TiO_2	1.97±0.01	3.4±1.0	8.0±4.6	-	-	-	2.737±0.01	3.3±1.1	6.8±1.8	-1.9±2.9	2.9
Pd2Ga/TiO_2	1.95±0.03	0.9±0.4	5.0	2.56±0.03	1.0	3.6±3.0	2.686±0.03	8.1±2.3	15.0±5.0	-8.7±2.2	2.0
Pd1Ga/TiO_2	1.98±0.02	1.5±0.3	3.0	-	-	-	2.736±0.018	5.3±1.1	8.5±1.7	-2.6±1.6	2.6
Pd0.5Ga/TiO_2	1.95±0.03	1.0±0.3	9.6±1.1	-	-	-	2.733±0.007	5.7±0.7	9.6±1.1	-5.0±0.9	1.6
Pd2In/TiO_2	-	-	-	-**	-**	-**	2.740±0.01	8.9±1.7	10.7±1.4	-3.7±1.6	1.6
Pd1In/TiO_2	1.99±0.02	2.5±0.7	5.5±3.5	-**	-**	-**	2.748±0.01	4.1±1.0	7.8±1.5	-0.9±1.8	1.6
Pd0.5In/TiO_2	2.01±0.01	3.0±0.6	6.9±2.7	-**	-**	-**	2.761±0.01	3.0±0.8	8.4±1.8	1.4±1.6	1.4

*Amplitude reduction factor determined as 0.78(CAT-ACT) and 0.88 (P64)
**In has a similar scattering factor to Pd and therefore is indistinguishable from Pd during EXAFS analysis

Table S.5. Catalytic activity of TiO_2 supported Pd-Ga and Pd-In catalysts towards the direct synthesis and subsequent degradation of H_2O_2

Catalyst	H_2 Conversion / %	H_2O_2 Selectivity /%	Productivity / $mol_{H2O2}kg_{cat}^{-1}h^{-1}$	H_2O_2 Concentration / wt.%	Degradation / $mol_{H2O2}kg_{cat}^{-1}h^{-1}$
Pd/TiO_2	57	24	103	0.21	1056
$Pd2Ga/TiO_2$	49	30	111	0.22	750
$Pd1Ga/TiO_2$	-	-	104	0.21	735
$Pd0.5Ga/TiO_2$	-	-	86	0.17	436
Ga/TiO_2	-	-	0	0	13
$Pd2In/TiO_2$	40	34	98	0.20	786
$Pd1In/TiO_2$	-	-	93	0.19	636
$Pd0.5In/TiO_2$	-	-	66	0.16	520
In/TiO_2	-	-	0	0	5

H_2O_2 direct synthesis reaction conditions: Catalyst (0.01 g), H_2O (2.9 g), MeOH (5.6 g), 5% H_2 / CO_2 (420 psi), 25% O_2 / CO_2 (160 psi), 0.5 h, 2 °C, 1200 rpm. **H_2O_2 degradation reaction conditions**: Catalyst (0.01 g), H_2O_2 (50 wt. % 0.68 g) H_2O (2.22 g), MeOH (5.6 g), 5% H_2 / CO_2 (420 psi), 0.5 h, 2 °C, 1200 rpm.

Table S.6. Comparison of the catalytic selectivity of bi-metallic Pd catalysts towards H_2O_2 as a function of secondary metal.

Reference	Catalyst	Reactor Type	Temp /	Pressure / bar	Time / h	Solvent	Promotor	H_2O_2 Selectivity / %
This work	Pd/TiO_2	Batch	2	40	0.5	H_2O/MeOH	-	24
	$Pd2Ga/TiO_2$	Batch	2	40	0.5	H_2O/MeOH	-	30
	$Pd2In/TiO_2$	Batch	2	40	0.5	H_2O/MeOH	-	34
Freakley[1]	1%Pd-4%Sn/SiO_2	Batch	2	40	0.5	H_2O/MeOH	-	95
	3%Pd-2%Sn/TiO_2	Batch	2	40	0.5	H_2O/MeOH	-	96
Ding[2]	3%Pd/TiO_2	Semi-batch	10	1	0.25	EtOH+H_2SO_4	0.12M H_2SO_4	54
	$Pd_{50}Sb/TiO_2$	Semi-batch	10	1	0.25	EtOH+H_2SO_4	0.12M H_2SO_4	73
Tian[3]	3%Pd/TiO_2	Semi-	10	1	0.17	EtOH+H_2SO_4	0.12M	65

	batch					H_2SO_4	
$Pd_{100}Te_1/TiO_2$	Semi-batch	10	1	0.17	$EtOH+H_2SO_4$	0.12M H_2SO_4	100

Table S.7. Leaching of Pd, In and Ga from supported catalysts in solvent after H_2O_2 synthesis reaction as determined by ICP-MS.

Catalyst	Pd / (wt. %)	Ga (wt. %)	In (wt. %)
Pd/TiO_2	0.02	-	-
$Pd2Ga/TiO_2$	0.2	0.4	-
$Pd1Ga/TiO_2$	0.02	0.1	-
$Pd0.5Ga/TiO_2$	0.1	0.1	-
$Pd2In/TiO_2$	0.1	-	0.06
$Pd1In/TiO_2$	0.01	-	0.001
$Pd0.5In/TiO_2$	0.1	-	0.002

H_2O_2 direct synthesis reaction conditions: Catalyst (0.01 g), H_2O (2.9 g), MeOH (5.6 g), 5% H_2 / CO_2 (420 psi), 25% O_2 / CO_2 (160 psi), 0.5 h, 2 °C, 1200 rpm

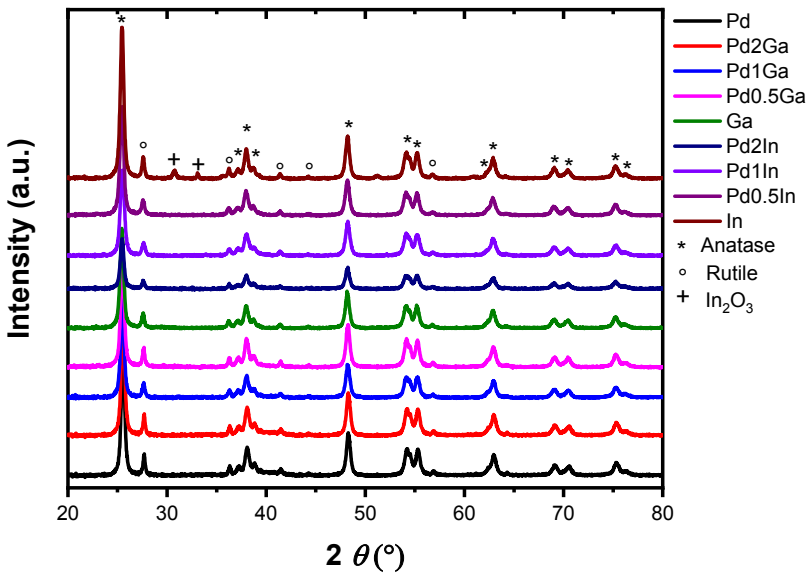

Figure S. 1. XRD patterns of TiO_2 supported Pd, Ga, In, Pd-Ga and Pd-In catalysts.

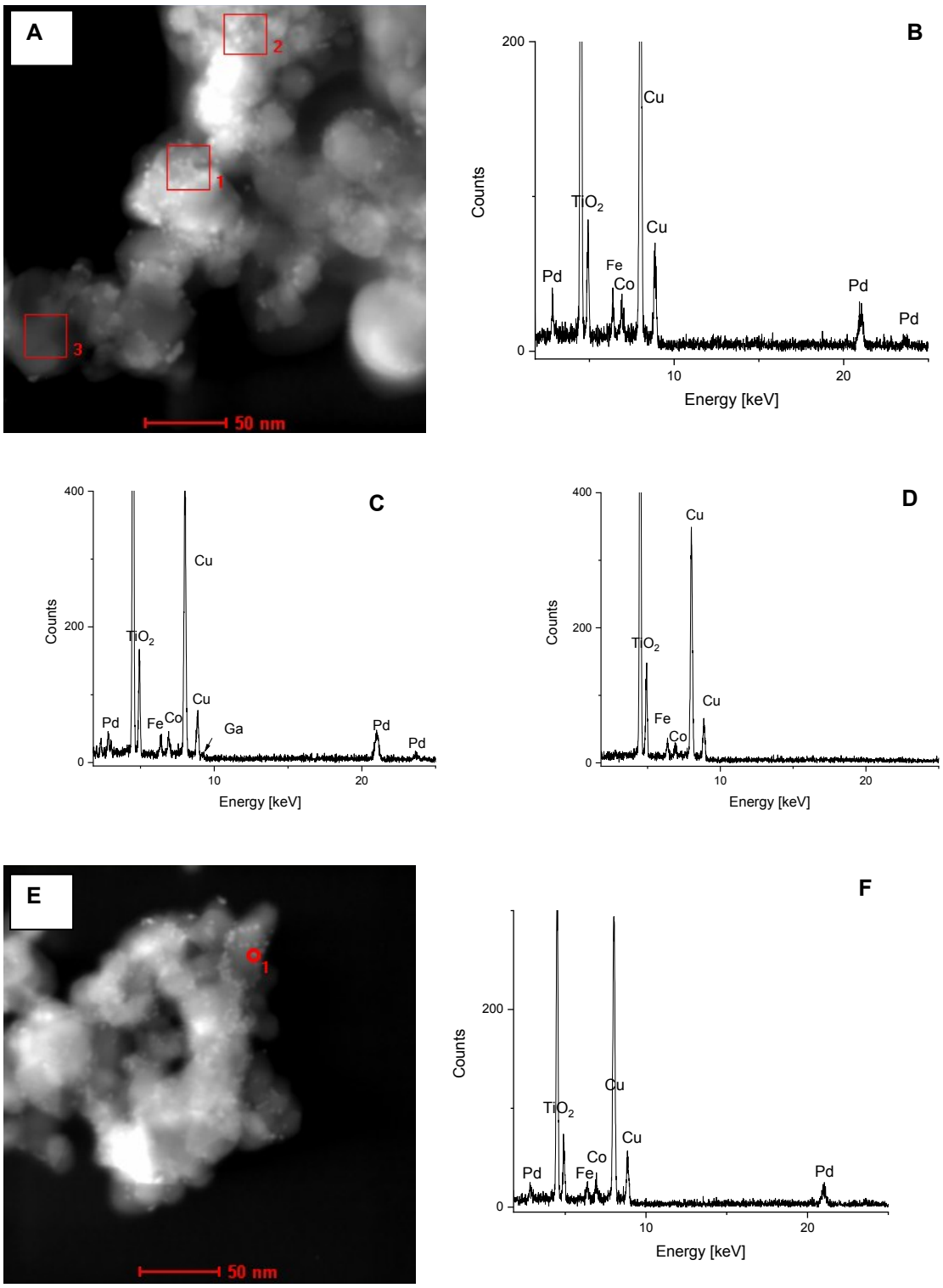

Figure S.2. A) STEM-HAADF image of Pd2Ga/TiO_2 and corresponding EDX spectra in B) area 1, C) area 2, and D) area 3. E) STEM-HAADF image of Pd2Ga/TiO_2 and corresponding EDX spectrum for a single Pd2Ga nanoparticle in F) point 1. In general, the overall EDX signal intensity of the Pd2Ga nanoparticles is very low (i.e. low Pd signal intensity while Ga could not be detected by EDX

analysis). (EDX spectra are enlarged for the 1.9-25 eV energy range; Cu is due to supporting TEM grid; Fe/Co refer to the pole shoe of the TEM).

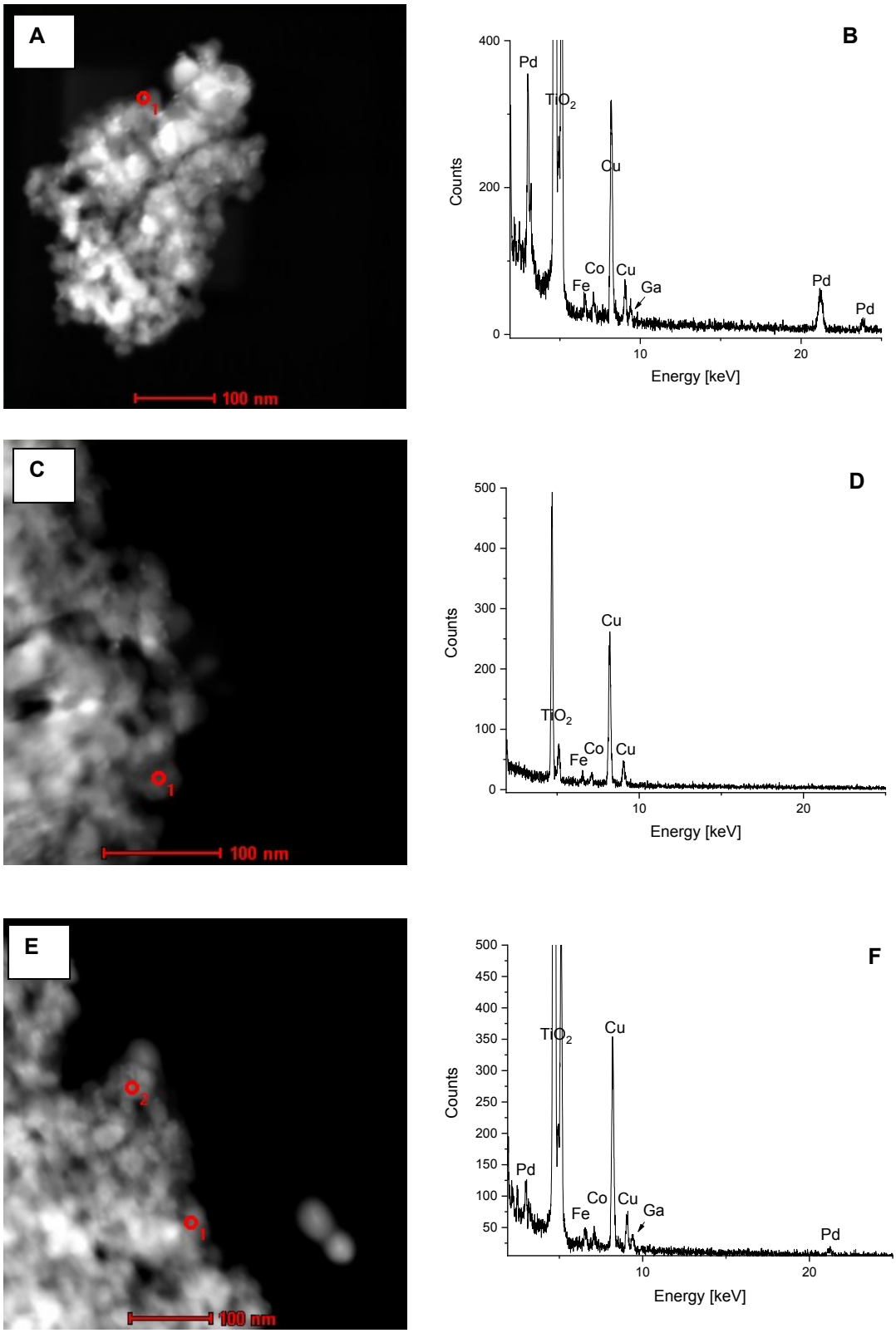

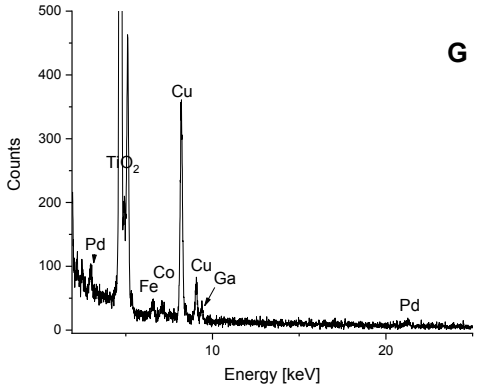

Figure S.3. A) STEM-HAADF image of PdGa2/TiO_2 and corresponding EDX spectrum in B) point 1. C) STEM-HAADF image of PdGa2/TiO_2 and corresponding EDX spectrum in D) point 1. E) STEM-HAADF image of PdGa2/s-TiO_2 and corresponding EDX spectrum in F) point 1 and G) point 2 (signals of very low intensity observed at 2.2 eV and 2.5 eV refer to P (P(octyl)$_3$ - nanoparticle ligands) and S (s-TiO_2), respectively). For PdGa2 nanoparticles, a Ga signal of low intensity is detected while there seems to be no Ga signal observed in the absence of Pd. However, it has to be noted that the distribution of some Ga over the support may not be completely excluded (EDX spectra are enlarged for the 1.9-25 eV energy range; Cu is due to supporting TEM grid; Fe/Co refers to the pole shoe of the TEM).

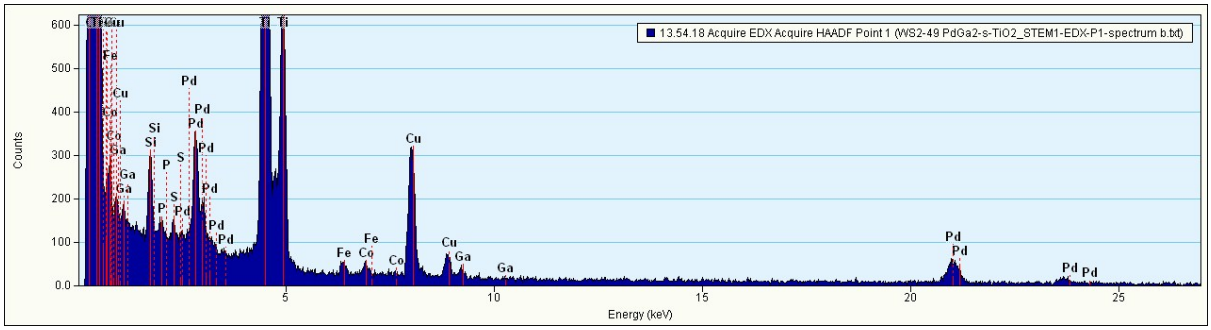

Figure S.4. EDX spectrum of PdGa2/TiO_2 (Figure S.3) in point 1 (B) above) indicating the peak positions.

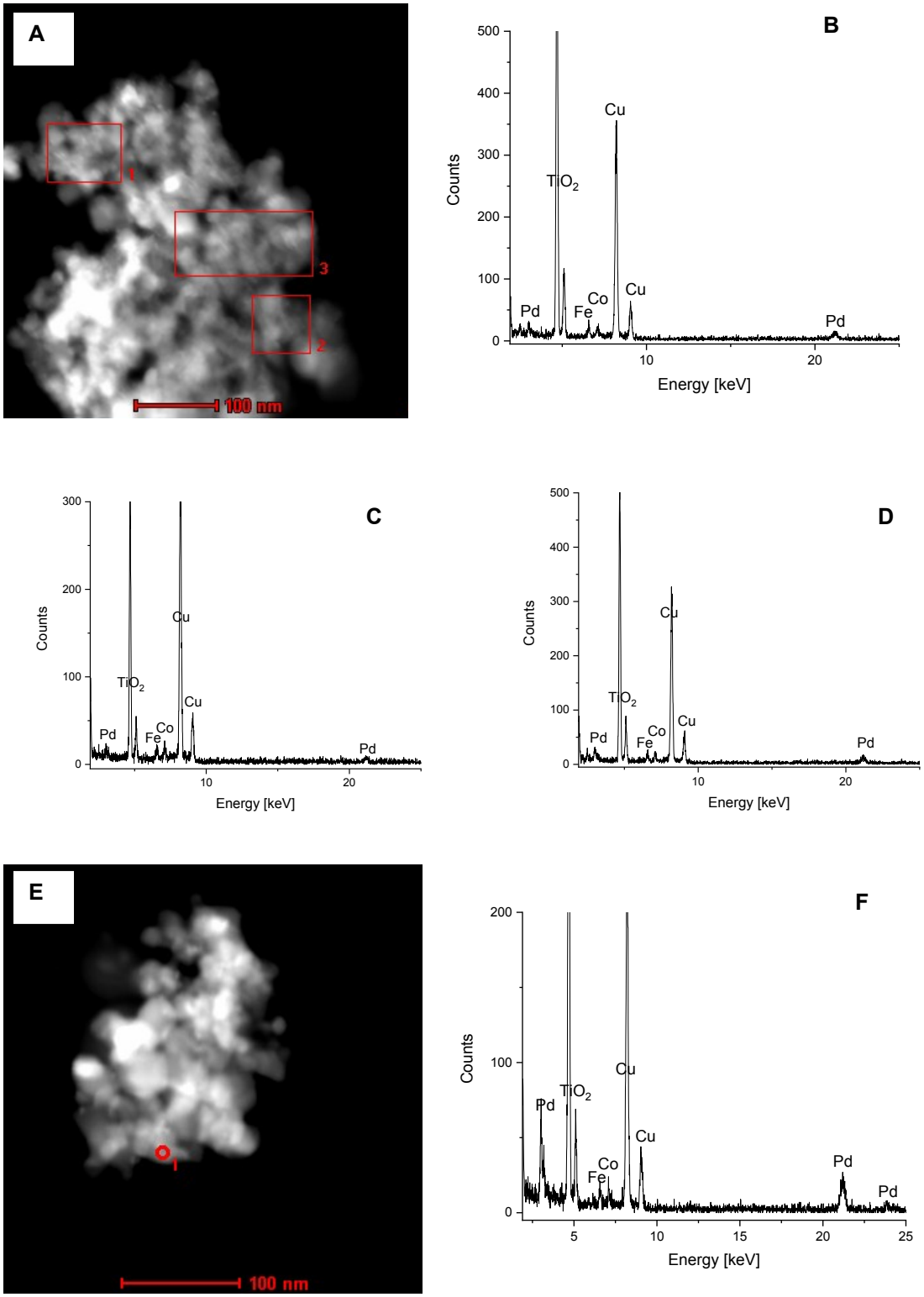

Figure S.5. A) STEM-HAADF image of Pd2In/TiO_2 and corresponding EDX spectra (enlarged for the 1.9-25 eV energy range) in B) area 1, C) area 2 and D) area 3. E) STEM-HAADF image of Pd2In/TiO_2 and corresponding EDX spectrum in F) point 1. Overall the EDX signal of the Pd2In nanoparticles is of very low intensity (i.e. low Pd signal intensity; In is not detected by EDX analysis). (EDX spectra are enlarged for the 1.9-25 eV energy range; Cu is due to supporting TEM grid; Fe/Co refers to the pole shoe of the TEM).

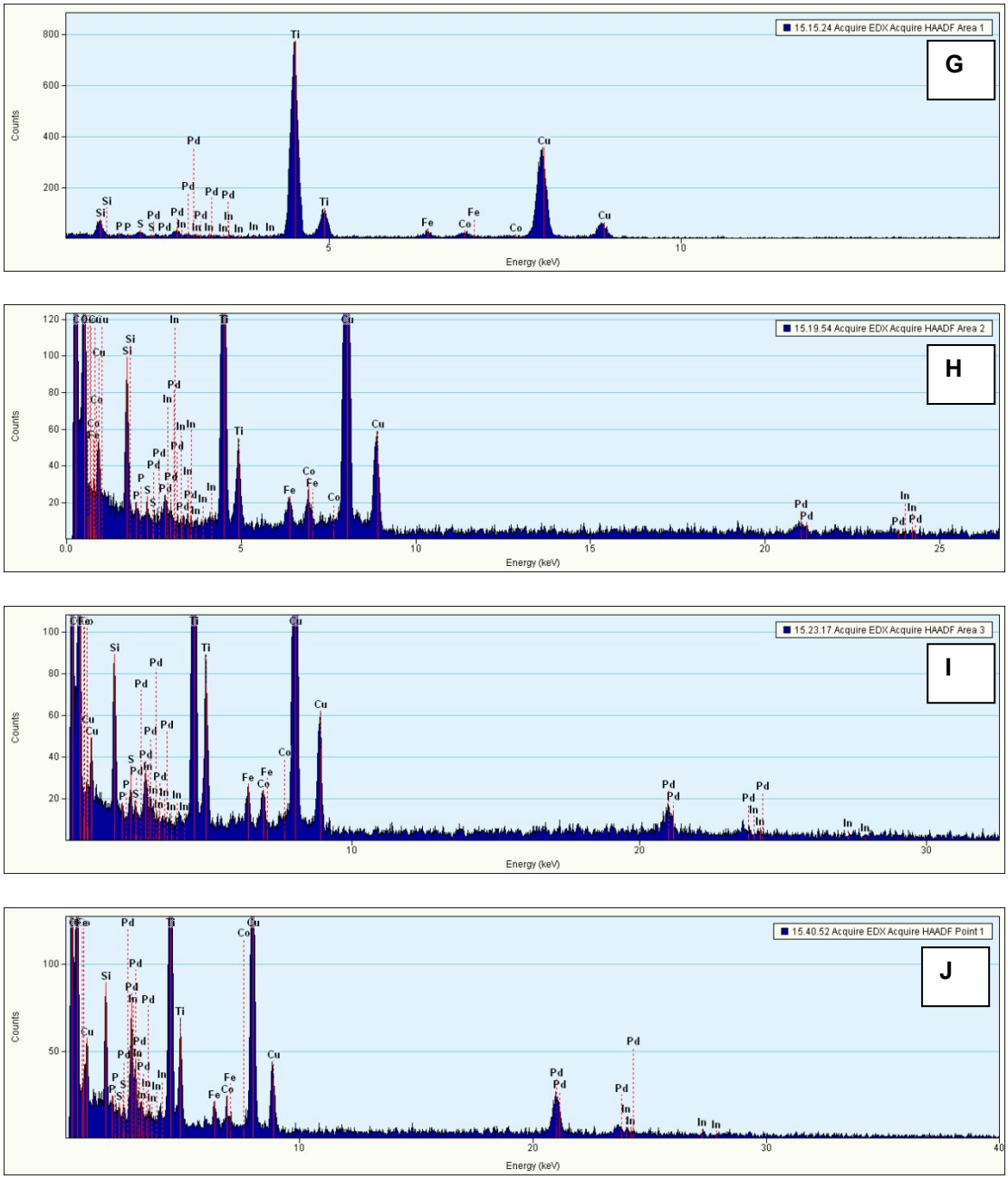

Figure S.6. EDX spectra of (Pd2In/s-TiO_2 in Figure S.5 in area 1 (G), area 2 (H), area 3 (I) and point 1(F) above) indicating the peak positions.

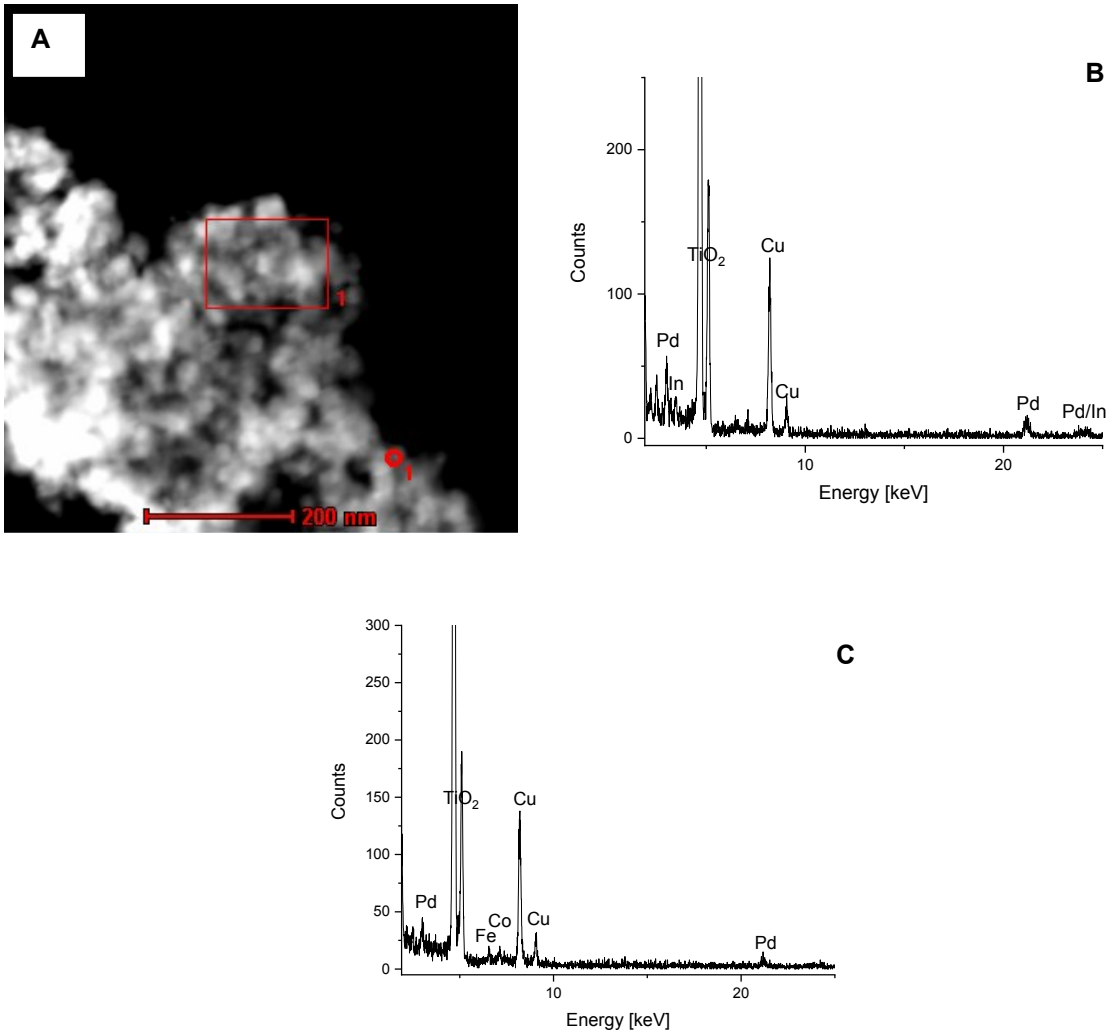

Figure S.7. A) STEM-HAADF image of PdIn2/TiO_2 and corresponding EDX spectra in B) area 1, C) area 2 and D) area 3. E) STEM-HAADF image of Pd2In/TiO_2 and corresponding EDX spectrum in F) point 1. Overall the EDX signal of the PdIn2 nanoparticles is of very low intensity (i.e. low Pd signal intensity; In is not detected by EDX analysis). (EDX spectra are enlarged for the 1.9-25 eV energy range; Cu is due to supporting TEM grid; Fe/Co refers to the pole shoe of the TEM).

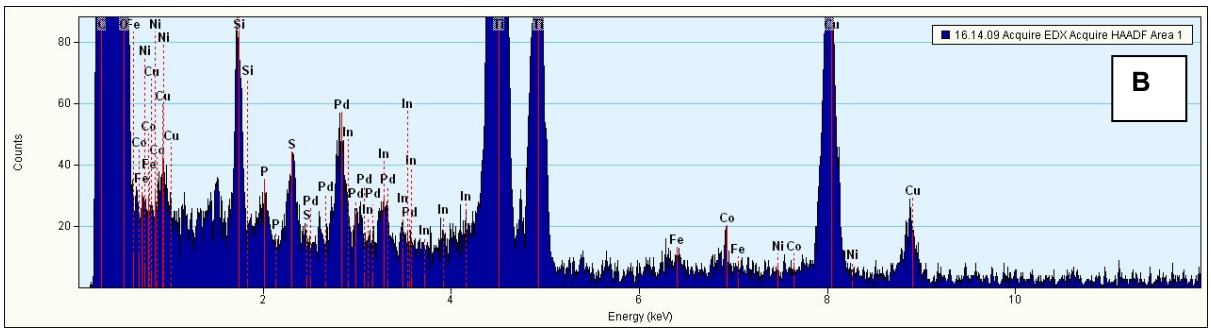

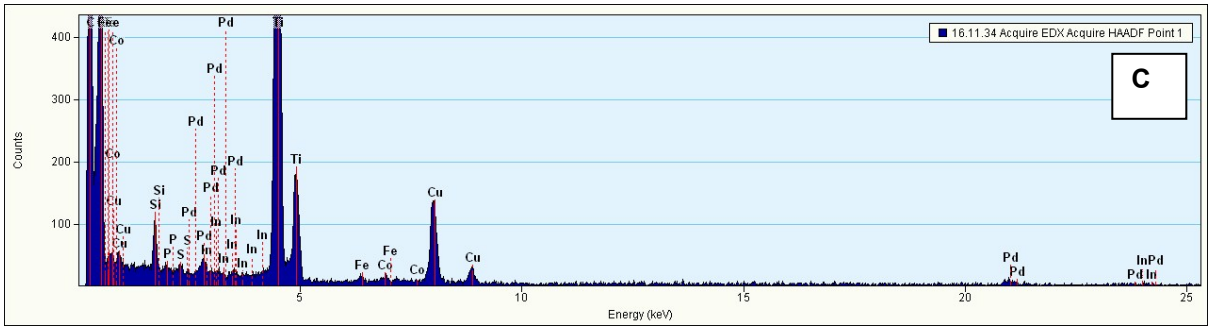

Figure S.8. EDX spectra of PdIn2/TiO_2 (Figure S.7 in area 1 (B) and point 1(C) above) indicating the peak positions.

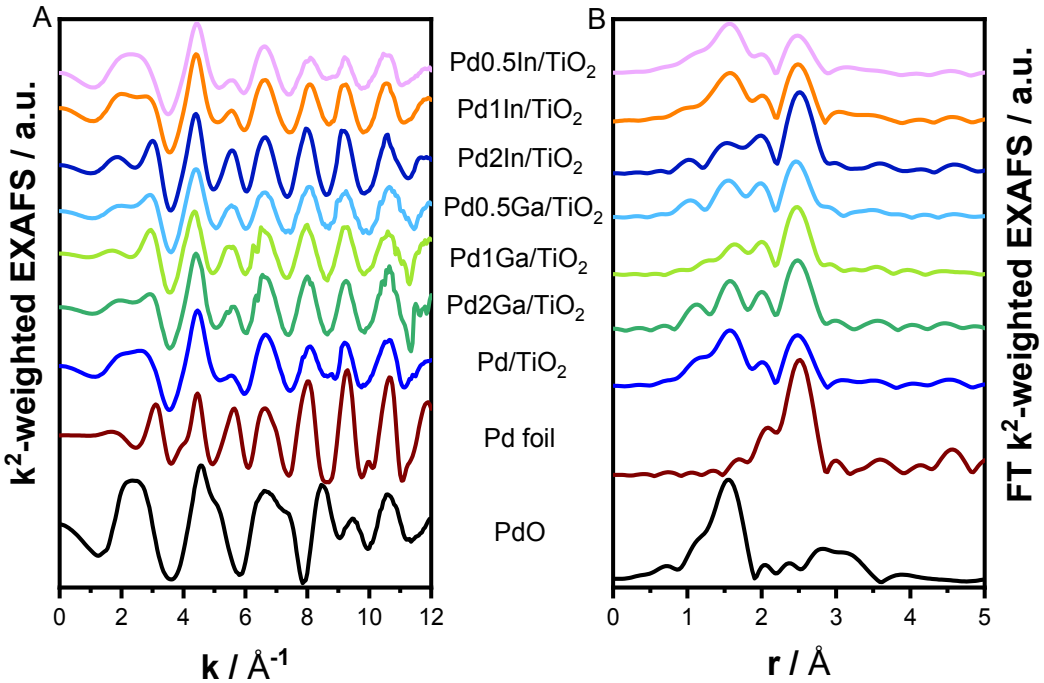

Figure S.9. A) k^2-weighted and B) Fourier-transformed k^2-weighted Pd-K edge EXAFS spectra (uncorrected for the phase shift) TiO_2 supported Pd, Ga, In, Pd-Ga and Pd-In catalysts as well as Pd (multiplied by 1/2) and PdO references.

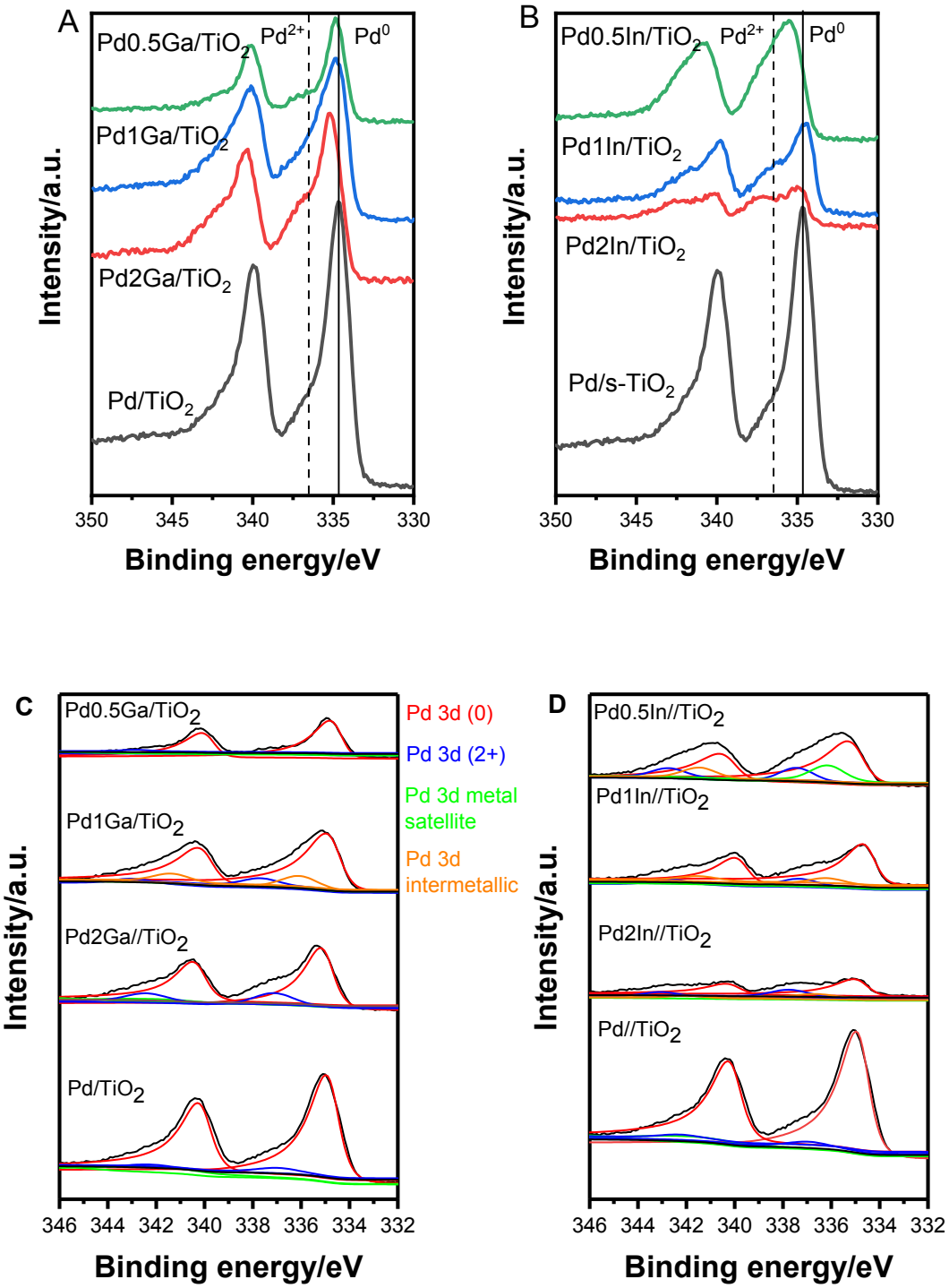
A
Pd0.5Ga/TiO2
Pd2+
Pd0
Pd1Ga/TiO2
Pd2Ga/TiO2
Pd/TiO2
Intensity/a.u.
350 345 340 335 330
Binding energy/eV
B
Pd0.5In/TiO2
Pd2+
Pd0
Pd1In/TiO2
Pd2In/TiO2
Pd/s-TiO2
Intensity/a.u.
350 345 340 335 330
Binding energy/eV
C
Pd0.5Ga/TiO2
Pd1Ga/TiO2
Pd2Ga//TiO2
Pd/TiO2
Pd 3d (0)
Pd 3d (2+)
Pd 3d metal satellite
Pd 3d intermetallic
Intensity/a.u.
346 344 342 340 338 336 334 332
Binding energy/eV
D
Pd0.5In//TiO2
Pd1In//TiO2
Pd2In//TiO2
Pd//TiO2
Intensity/a.u.
346 344 342 340 338 336 334 332
Binding energy/eV

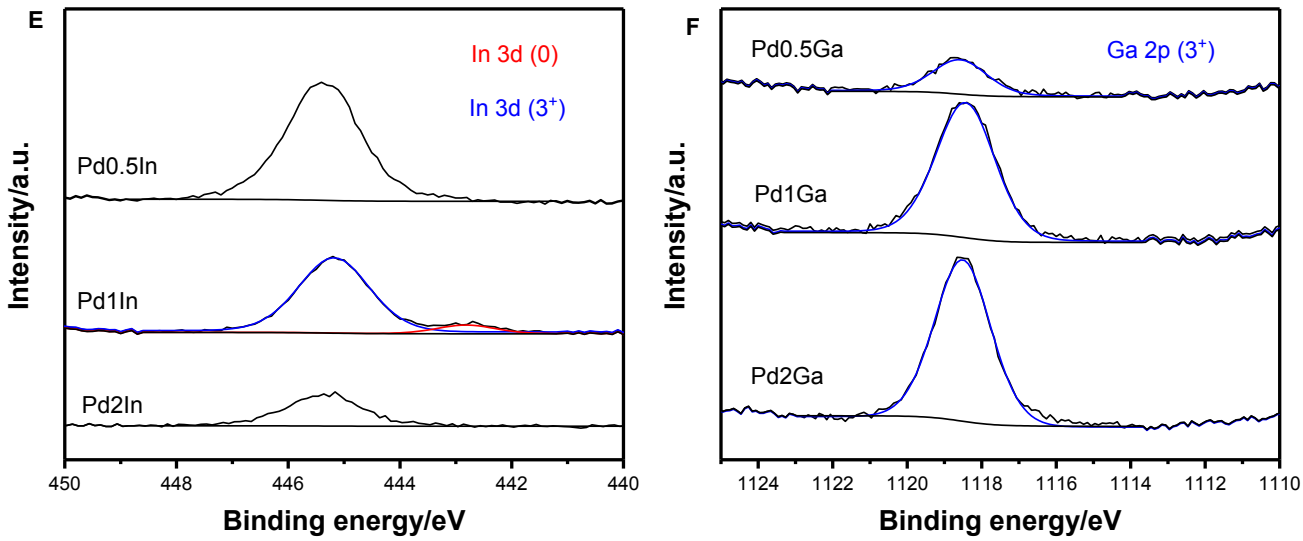

Figure S.10. XPS spectra of Pd 3d region for A) PdGa/TiO_2 and B) PdIn/TiO_2 catalysts with varying Pd: M ratio, with the corresponding deconvoluted spectra for the Pd region seen in C) for the PdGa/TiO_2 and D) for the PdIn/TiO_2 catalysts. Figure E) show XPS spectra for In 3d and Ga 2p regions for the corresponding PdM/TiO_2 catalysts.

For the monometallic Pd/TiO_2 catalyst, the Pd($3d_{5/2}$) binding energy is found to be 334.9 eV, consistent with metallic Pd[4], together with some Pd(II) around 337 eV. With the addition of Ga in Pd:Ga ratios of 2:1, 1:1 and 1:2 (Pd2Ga, Pd1Ga and Pd0.5Ga respectively), we note an initially higher binding energy for the metallic Pd peak, which systematically decreases with increasing Ga 335.1 eV to 334.7 eV. Interestingly, the Pd1Ga samples have a total of three Pd species, with binding energies of 334.8, 336.0 and 337.6 eV and attributed to Pd(0), PdGa intermetallic species and Pd(II) respectively.[2] The evidence, at least from XPS, for intermetallic formation in the Pd2Ga and Pd0.5Ga samples, is negligible.

For all samples, the Ga($2p_{3/2}$) binding energy is also found to vary upwards as the amount of Ga increases (1118.1 up to 1118.5 eV), the binding energy of which is consistent with Ga oxides and a consequence of contact of the samples with air.[3]

In respect of the PdIn catalysts, all samples exhibit an In($3d_{5/2}$) binding energy of 445 eV, *ca.* 1 eV higher than the energy characteristic of indium oxide[4, 5] and may be attributed to the surface oxide of a PdIn intermetallic species, of which there is evidence in the Pd(3d) spectra (see Figure S6 above), and together with prolonged X-ray exposure there is evidence of reduction of this surface species to reveal a smaller shoulder at 443 eV, consistent with intermetallic In phases.[5, 6]

References

1. S.J. Freakley, Q. He, J. H. Harrhy, L. Lu, D. A. Crole, D. J. Morgan, E. N. Ntainjua, J. K. Edwards, A. F. Carley, A. Y. Borisevich, C. J. Kiely and G. J. Hutchings, *Science*, 2016, **351**, 965-968.
2. D. Ding, X. Xu, P. Tian, X. Liu, J. Xu and Y. Han, *Chin. J. Catal*. 2018, **39**, 673–681.
3. P. Tian, X. Xu, C. Ao, D. Ding, W. Li, R. Si, W. Tu, J. Xu and Y. Han, *ChemSusChem* 2017, **10**, 3342–3346.
4. E. H. Voogt, A. J. M. Mens, O. L. J. Gijzeman and J. W. Geus, *Surf. Sci.*, 1996, **350**, 21-31.
5. K. Kovnir, M. Armbrüster, D. Teschner, T. Venkov, L. Szentmiklósi, F. C. Jentoft, A. Knop-Gericke, Y. Grin and R. Schlögl, *Surf. Sci.*, 2009, **603**, 1784-1792.
6. J. Osswald, R. Giedigkeit, R. E. Jentoft, M. Armbrüster, F. Girgsdies, K. Kovnir, T. Ressler, Y. Grin and R. Schlögl, *J. Catal.*, 2008, **258**, 210-218.
7. C. Rameshan, H. Lorenz, L. Mayr, S. Penner, D. Zemlyanov, R. Arrigo, M. Haevecker, R. Blume, A. Knop-Gericke and R. Schlögl, *J.Catal.*, 2012, **295**, 186-194.
8. A. Naumkin, A. Kraut-Vass, S. Gaarenstroom and C. Powell, *National Institute of Standards and Technology: Gaithersburg*, 2012.
9. A. García-Trenco, A. Regoutz, E. R. White, D. J. Payne, M. S. Shaffer and C. K. Williams, *Appl. Catal., B*, 2018, **220**, 9-18.